

Simultaneous measurements of all three components of velocity and vorticity vectors in a lobed jet flow by means of dual-plane stereoscopic particle image velocimetry

Cite as: Physics of Fluids 14, 2128 (2002); <https://doi.org/10.1063/1.1481741>

Submitted: 08 January 2002 • Accepted: 08 April 2002 • Published Online: 23 May 2002

Hui Hu, Tetsuo Saga, Toshio Kobayashi, et al.



View Online



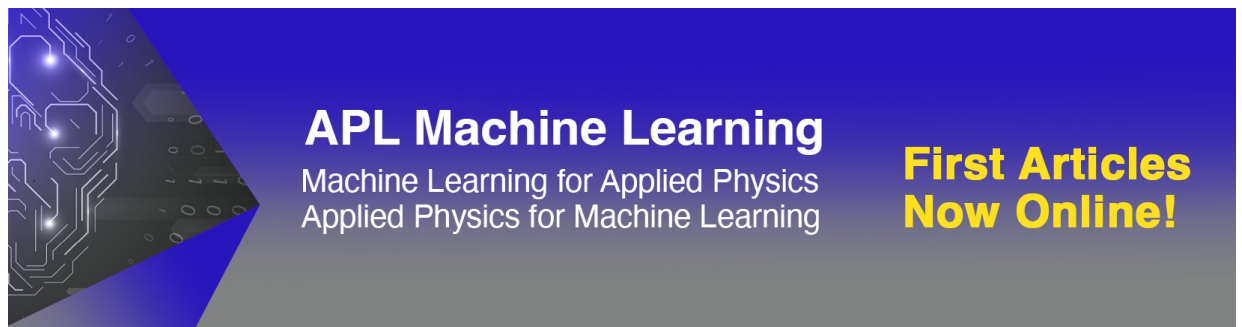
Export Citation

ARTICLES YOU MAY BE INTERESTED IN

[A study on a lobed jet mixing flow by using stereoscopic particle image velocimetry technique](#)
Physics of Fluids **13**, 3425 (2001); <https://doi.org/10.1063/1.1409537>

[Time-resolved stereoscopic particle image velocimetry investigation of the entrainment in the near field of circular and daisy-shaped orifice jets](#)
Physics of Fluids **22**, 035107 (2010); <https://doi.org/10.1063/1.3358465>

[An experimental study on the characteristics of wind-driven surface water film flows by using a multi-transducer ultrasonic pulse-echo technique](#)
Physics of Fluids **29**, 012102 (2017); <https://doi.org/10.1063/1.4973398>



APL Machine Learning
Machine Learning for Applied Physics
Applied Physics for Machine Learning

**First Articles
Now Online!**

Simultaneous measurements of all three components of velocity and vorticity vectors in a lobed jet flow by means of dual-plane stereoscopic particle image velocimetry

Hui Hu,^{a)} Tetsuo Saga, Toshio Kobayashi, and Nubuyuki Taniguchi

Institute of Industrial Science, University of Tokyo, Komaba 4-6-1, Meguro-Ku, Tokyo 153-8505, Japan

(Received 8 January 2002; accepted 8 April 2002; published 23 May 2002)

Results from an advanced particle image velocimetry (PIV) technique, named as dual-plane stereoscopic PIV technique, for making simultaneous measurements of all three components of velocity and vorticity vectors are presented for a lobed jet flow. The dual-plane stereoscopic PIV technique uses polarization conservation characteristic of Mie scattering to achieve simultaneous stereoscopic PIV measurements at two spatially separated planes. Unlike “classical” PIV systems or conventional stereoscopic PIV systems, which can only get one component of vorticity vectors, the present dual-plane stereoscopic PIV system can provide all three components of velocity and vorticity distributions in fluid flows instantaneously and simultaneously. The evolution and interaction characteristics of the large-scale streamwise vortices and azimuthal Kelvin–Helmholtz vortices in the lobed jet flow are revealed very clearly and quantitatively from the simultaneous measurement results of the dual-plane stereoscopic PIV system. A discussion about the satisfaction of the measurement results of the present dual-plane stereoscopic PIV system to mass conservation equation is also conducted in the present paper to evaluate the error levels of the measurement results. © 2002 American Institute of Physics. [DOI: 10.1063/1.1481741]

INTRODUCTION

Velocity and vorticity are two most important defining properties of turbulence, whether in development or in equilibrium. The simultaneous information revealed from velocity vector and vorticity vector distributions in fluid flows could help us very much to improve our understanding of complex flow phenomena. It is well known that the vorticity vector is defined as the curl of the velocity vector and can be expressed in the tensor notation in the Cartesian coordinate system as

$$\Omega_i = E_{i,j,k} \frac{\partial U_k}{\partial x_j}, \quad (1)$$

where $E_{i,j,k}$ is the alternating tensor and U_k is the velocity vector. Obviously, it is desirable to obtain all three components of the vorticity field simultaneously in order to gain a complete understanding of the instantaneous vorticity fields.

As a nonintrusive whole field measuring technique, particle image velocimetry (PIV)¹ is a most common used tool for conducting velocity field measurements of fluid flows. The simultaneous whole-field vorticity distributions can be obtained as the derivatives of the velocity vector fields obtained from PIV measurements. However, since “classical” PIV technique is a two-component, two-dimensional (2C–2D) measuring technique, which is only capable of obtaining two components of velocity vectors in an illuminated plane

instantaneously. Therefore, only one component of vorticity vectors can be obtained simultaneously as the measurement results of “classic” PIV systems.

Stereoscopic particle image velocimetry technique² always employs two cameras to record simultaneous but distinct off-axial views of the same region of interest (an illuminated plane within a fluid flow seeded with tracer particles). By doing view reconstruction, the corresponding image segments in the two views are matched to get all three components of flow velocity vectors. Compared with “classical” PIV technique, stereoscopic PIV technique can provide additional information about the out-of-plane velocity component simultaneously besides the two in-plane velocity components. However, from the view of vorticity vector measurement, it is still only one component of the vorticity vectors that can be obtained instantaneously from the measurement results of a conventional “single-plane” stereoscopic PIV system.

An advanced PIV technique, named as dual-plane stereoscopic PIV technique, will be described in the present paper for the simultaneous measurements of all three components of velocity and vorticity vector distributions in fluid flows. Unlike “classical” PIV systems or conventional “single-plane” stereoscopic PIV systems, the dual-plane stereoscopic PIV system described in the present study can provide all three components of velocity and vorticity vector distributions in fluid flows instantaneously and simultaneously.

The main technical aspects and system setup of the dual-plane stereoscopic PIV system will be described at first in the following context. Then, the measurement results of the

^{a)} Author to whom correspondence should be addressed. Present address: Turbulent Mixing and Unsteady Aerodynamics Laboratory, A22, Research Complex Engineering, Michigan State University, East Lansing, Michigan 48824. Electronic mail: huhui@egr.msu.edu

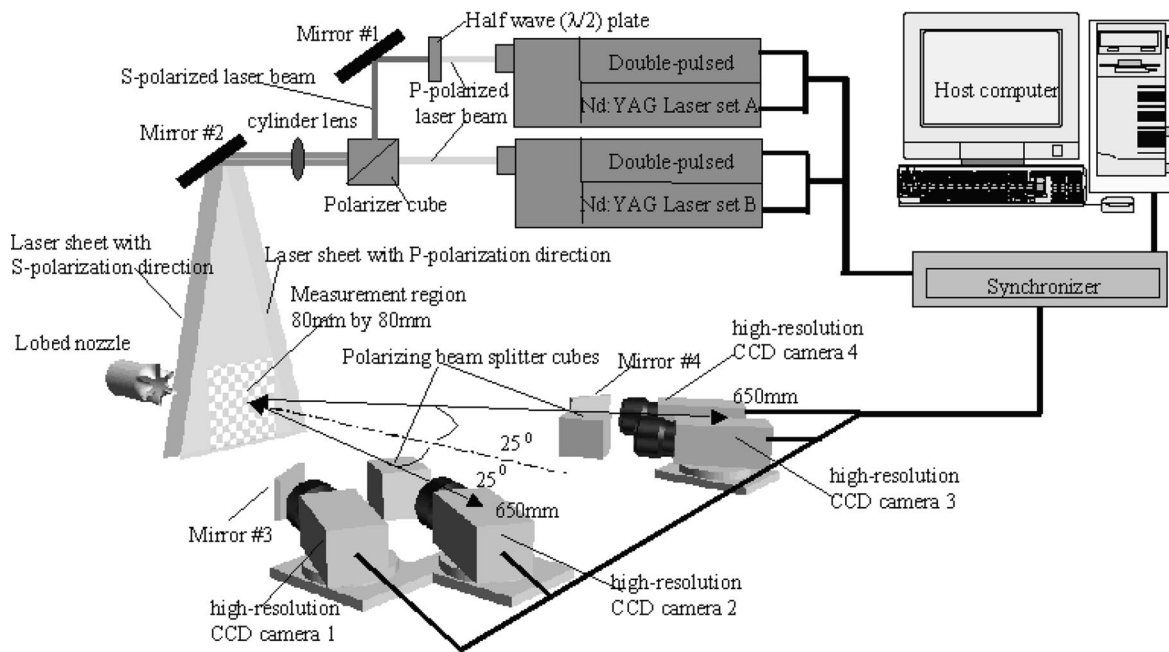


FIG. 1. The schematic setup of the dual-plane stereoscopic PIV system.

dual-plane stereoscopic PIV system in a lobed jet flow will be present to demonstrate the achievements of the simultaneous measurement of all three components of velocity and vorticity vectors. The evolution and interaction characteristics of the large-scale streamwise vortices and azimuthal Kelvin–Helmholtz vortices in the lobed jet flow will be discussed based on the simultaneous measurement results. A discussion about the satisfaction of the measurement results of the dual-plane stereoscopic PIV system to the mass conservation equation will also be given in the present paper to evaluate the error levels of the measurement results. The research described here represents, to our knowledge, the first quantitative, instantaneous and simultaneous measurement results of all three components of the velocity and vorticity vector distributions in a lobed jet flow. It is also believed to be the first to discuss the satisfaction of PIV measurement results to the mass conservation equation instantaneously and quantitatively.

DUAL-PLANE STEREOGRAPHIC PIV TECHNIQUE AND SYSTEM SETUP

It is well known that particle scattering can be either Mie scattering or Rayleigh scattering depending on the relative diameter of the particles compared with the wavelength (λ) of the incident light. According to McCartney,³ Mie scattering is generally defined as scattering from particles which is greater than $1/10$ of the incident light wavelength (λ), while Rayleigh scattering is defined as scattering from particles with diameters less than $1/10\lambda$. Most of the PIV systems work in the Mie scattering regime.

In the Mie scattering regime, the scattering will have a dominant forward direction, and nonuniform “lobed” scattering towards the sides. The scattering distributions will depend upon the particle size, the wavelength and polarization of incident light. It should be noted that the polarization di-

rection of Mie scattering is conservative under certain conditions. If the incident light is linearly polarized, the light scattered from small particles ($\sim 1 \mu\text{m}$ in diameter) maintains the polarization of the incident light. Further discussions about the polarization conservation of Mie scattering can be found from Ref. 4. As the same as Keahler and Kompenhans,⁵ the dual-plane stereoscopic PIV system described in the present paper utilizes the polarization conservation characteristic of Mie scattering to do separation of the scattered light from two illuminating laser sheets with orthogonal polarization direction in order to achieve simultaneous stereoscopic PIV measurements at two spatially separated planes.

Figure 1 shows the schematic setup of the dual-plane stereoscopic PIV system used in the present study. Two sets of widely used double-pulsed Nd:YAG lasers (New Wave, 50 mJ/pulse, $\lambda=532 \text{ nm}$) with additional optics (half wave plate, mirrors, polarizer, and cylindrical lens) were used to setup the illumination system of the dual-plane stereoscopic PIV system. The *P*-polarized laser beams from the double-pulsed Nd:YAG laser set *A* is turned into *S*-polarized light by passing a half wave ($\lambda/2$) plate before they are combined with the *P*-polarized laser beams from the double-pulsed Nd:YAG laser set *B*. The *P*-polarized laser beams from the laser set *B* transmit through the Polarizer cube, while the *S*-polarized light from the double-pulsed Nd:YAG laser set *A* are reflected by the Polarizer cube. By adjusting the angle and/or the location of mirror #1, the laser beams from the laser set *A* and laser set *B* can be overlapped or not. Passing through a set of cylindrical lenses and reflected by mirror #2, the laser beams are expanded into two paralleling laser sheets with orthogonal polarization to illuminate the studied flow field at two spatially separated planes or overlapped at

one plane. In the present study, the thickness of the illuminating laser sheets is about 2.0 mm, and the gap between the centers of the two illuminating laser sheets is adjusted as 2.0 mm.

Two pairs of high-resolution CCD cameras with polarizing beam splitter cubes and mirrors were used to capture the stereoscopic PIV images simultaneously at the two measurement planes illuminated by the two laser sheets with orthogonal linear polarization. The two pairs of the high-resolution CCD cameras (1 K by 1 K, TSI PIVCAM 10–30) were settled on an optical table with a pair of polarizing beam splitter cubes and two high reflectivity mirrors installed in front of the cameras to separate the scattered light from the two illuminating laser sheets with orthogonal linear polarization. The illuminating laser light with orthogonal linear polarization is scattered by the tracer particles seeded in the objective fluid flow. Due to the polarization conservation characteristic of Mie scattering, the scattered light from the *P*-polarized laser sheet will keep the *P*-polarization direction and pass straight through the polarizing beam-splitter cubes and is detected by camera 2 and camera 3. The scattered light from the *S*-polarized laser sheet will keep the *S*-polarization direction and emerge from the polarizing beam splitter cubes at the right angles to the incident direction. Reflected by the two high reflectivity mirrors (mirror #3 and #4), the scattered *S*-polarized light is detected by camera 1 and camera 4.

The two pairs of high-resolution CCD cameras were arranged in an angular displacement configuration in order to get a large measurement window. With the installation of tilt-axis mounts, the lenses and camera bodies were adjusted to satisfy Scheimpflug condition⁶ to obtain focused particle images everywhere in the image recording planes. In the present study, the distance between the illuminating laser sheets and image recording planes of the CCD cameras is about 650 mm, and the angle between the view axes of the cameras is about 50°. For such arrangement, the size of the stereoscopic PIV measurement windows is about 80 mm by 80 mm.

The CCD cameras and double-pulsed Nd:YAG laser sets were connected to a workstation (host computer) via a synchronizer (TSI LaserPulse synchronizer), which controlled the timing of the laser sheet illumination and the CCD camera data acquisition. In the present study, the time interval between the two pulsed illuminations of each double-pulsed Nd:YAG laser set was set as 30 μ s.

A general three-dimensional (3D) *in situ* calibration procedure⁷ was conducted in the present study to obtain the mapping functions between the image planes and object planes. A target plate (100 mm by 100 mm) with 100 μ m diameter dots spaced at the interval of 2.5 mm was used for the 3D *in situ* calibration. The front surface of the target plate was aligned with the centers of the laser sheets, and then calibration images were captured at several locations across the depth of the laser sheets. The space interval between these locations was 0.5 mm for the present study. The 3D mapping function used in the present study was taken to be a multidimensional polynomial, which is fourth order for the directions (*X* and *Y* directions) paralleling the laser sheet planes and second order for the direction (*Z* direction) nor-

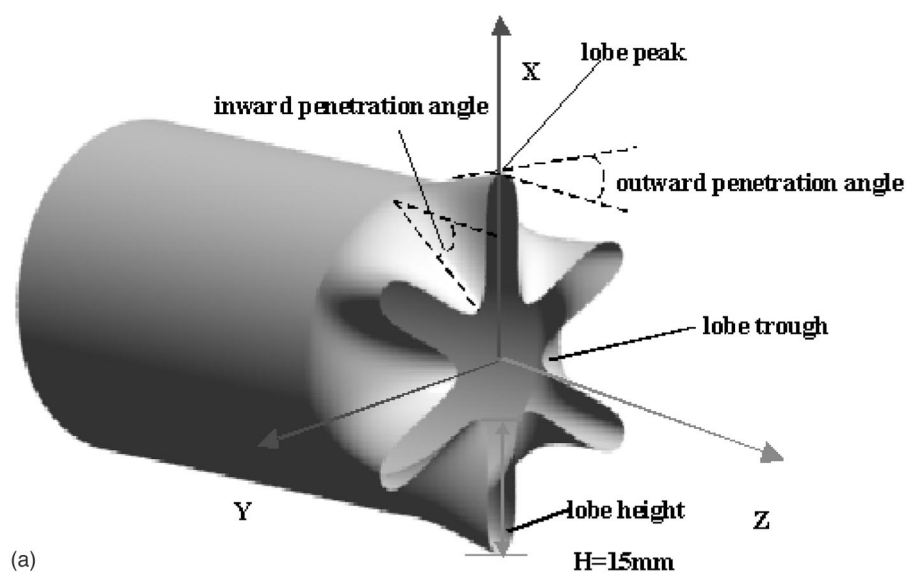
mal to the laser sheet planes. The coefficients of the multidimensional polynomial were determined from the calibration images by using a least-square method. The two-dimensional particle image displacements in each image plane was calculated separately by using a hierarchical recursive PIV (HR-PIV) software developed “in-house.” The HR-PIV software is based on hierarchical recursive processes of conventional spatial correlation operation with off-setting of the displacements estimated by the former iteration step, and hierarchical reduction of the interrogation window size and search distance in the next iteration step.⁸ Compared with conventional cross-correlation based PIV image processing methods, the hierarchical recursive PIV method has advantages in the spurious vector suppression and spatial resolution improvement of PIV result.

Finally, by using the mapping functions obtained by the 3D *in situ* calibration and the two-dimensional displacements in each image planes, all three components of the velocity vectors in the two illuminating laser sheet planes were reconstructed. Further details about the system setup, 3D *in situ* calibration and image processing of the present dual-plane stereoscopic PIV system can be found from Refs. 9 and 10.

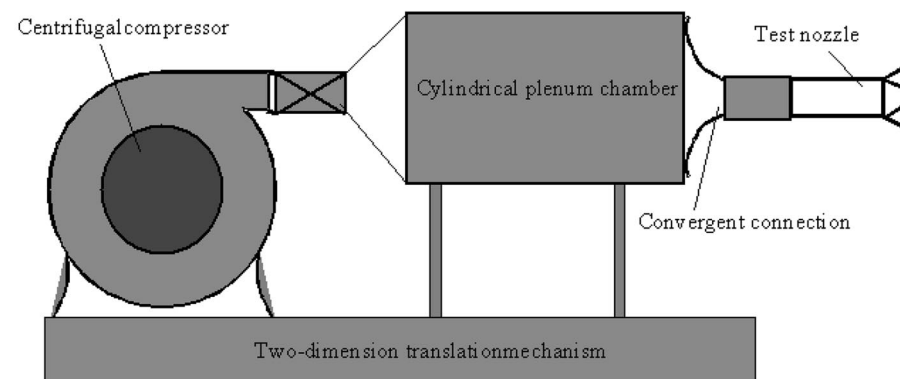
LOBED JET FLOW AND EXPERIMENTAL APPARATUS

A lobed nozzle, which consists of a splitter plate with convoluted trailing edge, is considered a very promising fluid mechanic device for efficient mixing of two co-flow streams with different velocity, temperature and/or species. The large-scale streamwise vortices generated by lobed nozzles and azimuthal vortices due to the Kelvin–Helmholtz instability have been suggested to play important roles in the mixing processes of lobed mixing flows.^{11,12} Since most of previous studies on lobed mixing flows were conducted by using conventional measurement techniques like Pitot probes, hot film anemometer and laser doppler velocimetry, instantaneous, quantitative whole-field velocity and vorticity distributions in lobed mixing flows have never been obtained until the recent work of the authors.^{13,14} In the earlier work of the authors, planar laser induced fluorescence (PLIF) and “classical” PIV techniques¹³ and conventional “single-plane” stereoscopic PIV technique¹⁴ were used to study lobed jet mixing flows. Based on the directly perceived PLIF flow visualization images and quantitative velocity, vorticity and turbulence intensity distributions of the PIV measurement results, the evolution and interaction characteristics of various vortical and turbulent structures in lobed jet mixing flows were discussed.

The measurement results obtained in the earlier works of the authors are from a “classical” PIV system and a conventional “single-plane” stereoscopic PIV system. Only the streamwise vortical structures or the azimuthal Kelvin–Helmholtz vortical structures in the lobed jet flows can be revealed instantaneously from the measurement results. Since the present dual-plane stereoscopic PIV system can provide all three components of velocity and vorticity vector distributions simultaneously, the large-scale streamwise vortices and azimuthal Kelvin–Helmholtz vortical structures in lobed mixing flows can be revealed simultaneously from the



(a)



(b)

FIG. 2. The lobed nozzle and experimental rig used in the present study. (a) Lobed nozzle. (b) Experimental rig.

measurement results. The simultaneous information will be very helpful to understand the evolution and interaction characteristics of the streamwise vortices and azimuthal Kelvin–Helmholtz vortical structures in the lobed mixing flows.

Figure 2(a) shows the geometry parameters of the lobed nozzle used in the present study. The lobed nozzle has six lobes. The width of each lobe is 6 mm and the height of each lobe is 15 mm ($H=15$ mm). The inward and outward penetration angles of the lobed structures are $\theta_{in}=22^\circ$ and $\theta_{out}=14^\circ$, respectively. The diameter of the lobed nozzle is 40 mm ($D=40$ mm).

Figure 2(b) shows the jet flow experimental rig used in the present study. A centrifugal compressor was used to supply the air jet. A cylindrical plenum chamber with honeycomb structures was used for settling the airflow. Through a convergent connection (convergent ratio is about 50:1), the airflow is exhausted from the test nozzle. The velocity range of the air jet out of the convergent connection (at inlet of the test nozzle) could be varied from 5 to 35 m/s. In the present study, a mean speed of the air jet at the inlet of the lobed nozzle of $U_0=20.0$ m/s was used. The corresponding Reynolds number is 5.517×10^5 based on the nozzle diameter. The air jet flow was seeded with 1–5 μm DEHS (Di-2-EthylHexyl-Sebact) droplets generated by a seeding

generator.¹⁵ The DEHS droplets out of the seeding generator were divided into two streams; one is used to seed the core jet flow and the other for ambient air seeding.

SIMULTANEOUS MEASUREMENT RESULTS OF ALL THREE COMPONENTS OF VELOCITY AND VORTICITY VECTORS

A pair of typical instantaneous measurement results of the dual-plane stereoscopic PIV system in two parallel cross planes ($Z=10$ mm and $Z=12$ mm) near to the trailing edge of the lobed nozzle is shown in Fig. 3. Since the characteristics of the mixing process in lobed mixing flows revealed from velocity distributions have been discussed intensively in the earlier work of the authors,^{13,14} the results and discussions given in the present paper will mainly focus on the simultaneous measurement results of all three components of vorticity distributions to reveal the evolution and interaction characteristics of various vortical and turbulent structures in the lobed jet flow.

According to the definition of vorticity vector given in Eq. (1), the three components of normalized vorticity vectors in the lobed jet flow can be expressed by following equations:

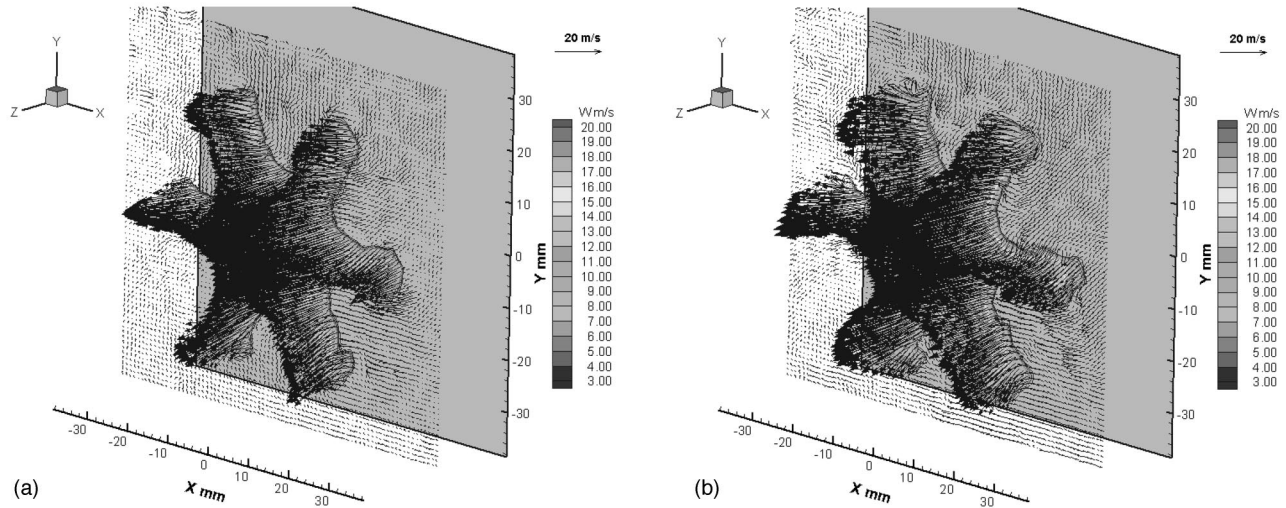


FIG. 3. A pair of typical instantaneous measurement results of the dual-plane stereoscopic PIV system. (a) Instantaneous velocity field in the $Z = 10$ mm cross plane. (b) Simultaneous velocity field in the $Z = 12$ mm cross plane.

$$\varpi_x = \frac{D}{U_0} \left(\frac{\partial w}{\partial y} - \frac{\partial v}{\partial z} \right), \quad (2)$$

$$\varpi_y = \frac{D}{U_0} \left(\frac{\partial u}{\partial z} - \frac{\partial w}{\partial x} \right), \quad (3)$$

$$\varpi_z = \frac{D}{U_0} \left(\frac{\partial v}{\partial x} - \frac{\partial u}{\partial y} \right), \quad (4)$$

where D is the diameter of the lobed nozzle, and U_0 is the velocity of the jet flow at the nozzle inlet. While, u , v , and w are the instantaneous velocity in X , Y , and Z directions (Fig. 2).

It should be noted that the terms like $\partial u/\partial z$ and $\partial v/\partial z$ in the above equations cannot be determined from the measurement results of a “classical” PIV system or a conventional “single-plane” stereoscopic PIV system. Therefore, only the out-of-plane component (ϖ_z) of the vorticity vector can be obtained instantaneously from the measurement results. Since the present dual-plane stereoscopic PIV system can provide the velocity fields (all three components) at two illuminated planes simultaneously, all the terms in the above vorticity definition equations can be determined. Besides the out-of-plane component ϖ_z , the other two in-plane components of the vorticity vectors (ϖ_x and ϖ_y) can be obtained in either of the two illuminated planes with first-order approximation, and in the central plane between the two parallel illuminated planes with second-order approximation accuracy. Based on the simultaneous velocity distributions in $Z = 10$ mm and $Z = 12$ mm cross planes given in Fig. 3, all the three components of the instantaneous vorticity distributions in the $Z = 10$ mm cross plane were calculated. The results are shown in Figs. 4(a), 4(b), and 4(c).

As described previously, there are two kinds of vortical structures are very important for the mixing process in lobed mixing flows. One is the large-scale streamwise vortices generated by the special geometry of lobed nozzle. The other is the azimuthal vortices rolled up at the interface of shear lay-

ers due to the Kelvin–Helmholtz instability. For the large-scale streamwise vortices generated by the special trailing edge of the lobed nozzle, their existence were revealed very clearly from the instantaneous streamwise vorticity distribution shown in Fig. 4(c). In order to reveal the azimuthal vortices in the lobed jet flow due to the Kelvin–Helmholtz instability, the x component and y component of the vorticity vectors were combined into in-plane (azimuthal) vorticity by using the following equation:

$$\varpi_{\text{in-plane}} = \sqrt{\varpi_x^2 + \varpi_y^2}. \quad (5)$$

The distribution of the in-plane (azimuthal) vorticity in the $Z = 10$ mm cross plane of the lobed jet flow is given in Fig. 4(d). As it is expected, the azimuthal Kelvin–Helmholtz vortices was found to be a vortex ring, which has the same geometry as the lobed trailing edge at the exit of the lobed nozzle.

The ensemble-averaged streamwise vorticity and azimuthal (in-plane) vorticity distributions in the lobed jet flow at $Z = 10$ mm cross plane were calculated based on 400 instantaneous measurement results, which are given in Figs. 4(e) and 4(f). Compared with the instantaneous streamwise and azimuthal vorticity distributions, the iso-vorticity contours of the ensemble-averaged streamwise and azimuthal vortices were found much smoother. However, they have almost the same distribution patterns and magnitudes as their instantaneous counterparts, which may indicate that the generations of the streamwise vortices and azimuthal vortex ring at the exit of the lobed nozzle are quite steady.

Figure 5 shows the simultaneous measurement results of the dual-plane stereoscopic PIV system in the $Z = 40$ mm ($Z/D = 1.0$, $Z/H = 2.67$) cross plane of the lobed jet flow. Compared with that at the exit of the lobed nozzle, the lobed jet flow has become much more turbulent. However, the “signature” of the lobed nozzle in a form of “six-lobe structure” can still be identified in the instantaneous and ensemble-averaged velocity fields [Figs. 5(a) and 5(b)]. The

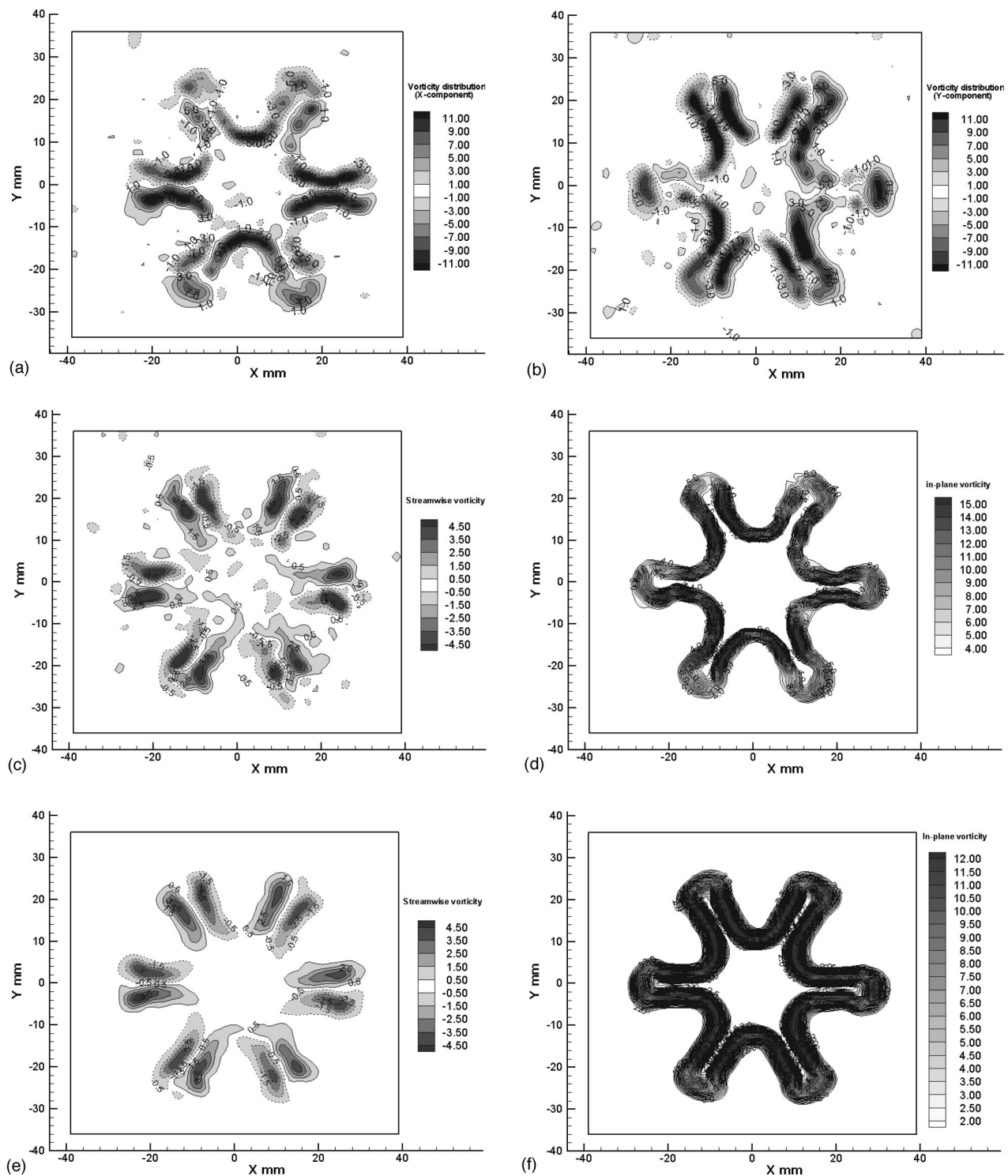


FIG. 4. All three components of the vorticity vector distributions in the $Z = 10$ mm ($Z/D = 0.25$) cross plane of the lobed jet flow. (a) Instantaneous vorticity (X component), (b) simultaneous vorticity (Y component), (c) simultaneous streamwise vorticity (Z component) distribution, (d) simultaneous azimuthal (in-plane) vorticity distribution, (e) ensemble-averaged streamwise vorticity distribution, (f) ensemble-averaged azimuthal (in-plane) vorticity distribution.

six pairs of counter-rotating streamwise vortices generated by the lobed nozzle were found to deform very serious in the instantaneous streamwise vorticity distribution [Fig. 5(c)]. Some of the large-scale streamwise vortices were found to break into smaller vortices. From the ensemble-averaged streamwise vorticity distribution shown in Fig. 5(d), the six pairs of ensemble-averaged streamwise vortices were found

to expand radially. The strength of these ensemble-averaged streamwise vortices were found to decrease very much with the maximum value of the ensemble-averaged streamwise vorticity only about the half of that at the exit of the lobed nozzle.

From the instantaneous azimuthal vorticity distribution given in Fig. 5(e), it can be seen that the azimuthal vortical

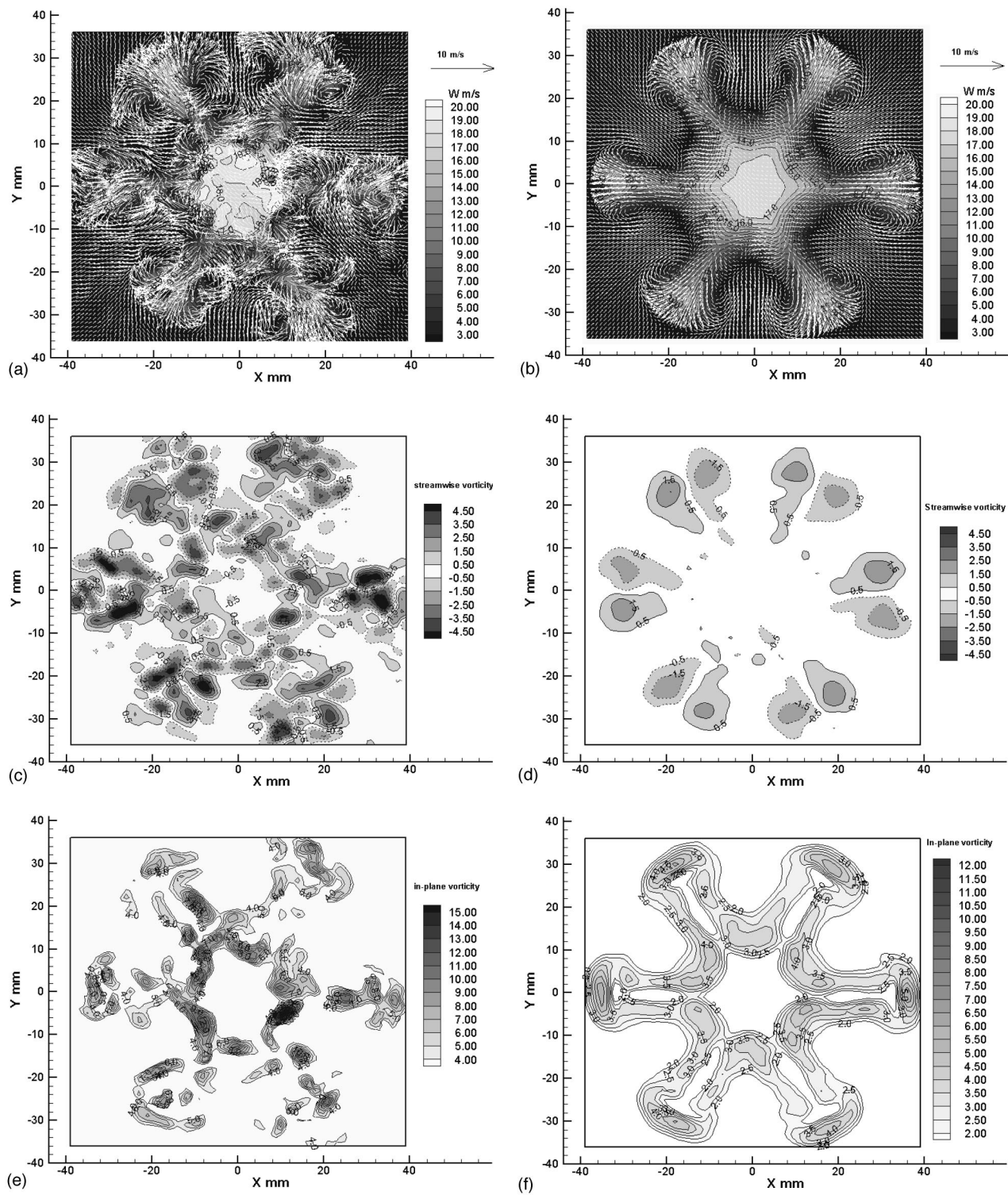


FIG. 5. The measurement results of the dual-plane stereoscopic PIV system in the $Z=40$ mm ($Z/D=1.0$) cross plane of the lobed jet flow. (a) Instantaneous velocity distribution, (b) ensemble-averaged velocity distribution, (c) simultaneous streamwise vorticity distribution, (d) ensemble-averaged streamwise vorticity distribution, (e) simultaneous azimuthal (in-plane) vorticity distribution, (f) ensemble-averaged azimuthal (in-plane) vorticity distribution.

ring, which has the same geometry as the nozzle trailing edge at the exit of the lobed nozzle, has broken into many disconnected vortical tubes in this cross plane. The broken azimuthal vortical fragments at the lobe troughs were found to connect again to form a new circular-ring-like structure in the center of the lobed jet flow.

Based on qualitative flow visualization results, McCormick and Bennett¹¹ suggested that the streamwise vortices would deform the azimuthal Kelvin–Helmholtz vortical tubes into pinch-off structures due to the interaction between the streamwise vortices and azimuthal Kelvin–Helmholtz vortical tubes. Such pinched-off effect is revealed very

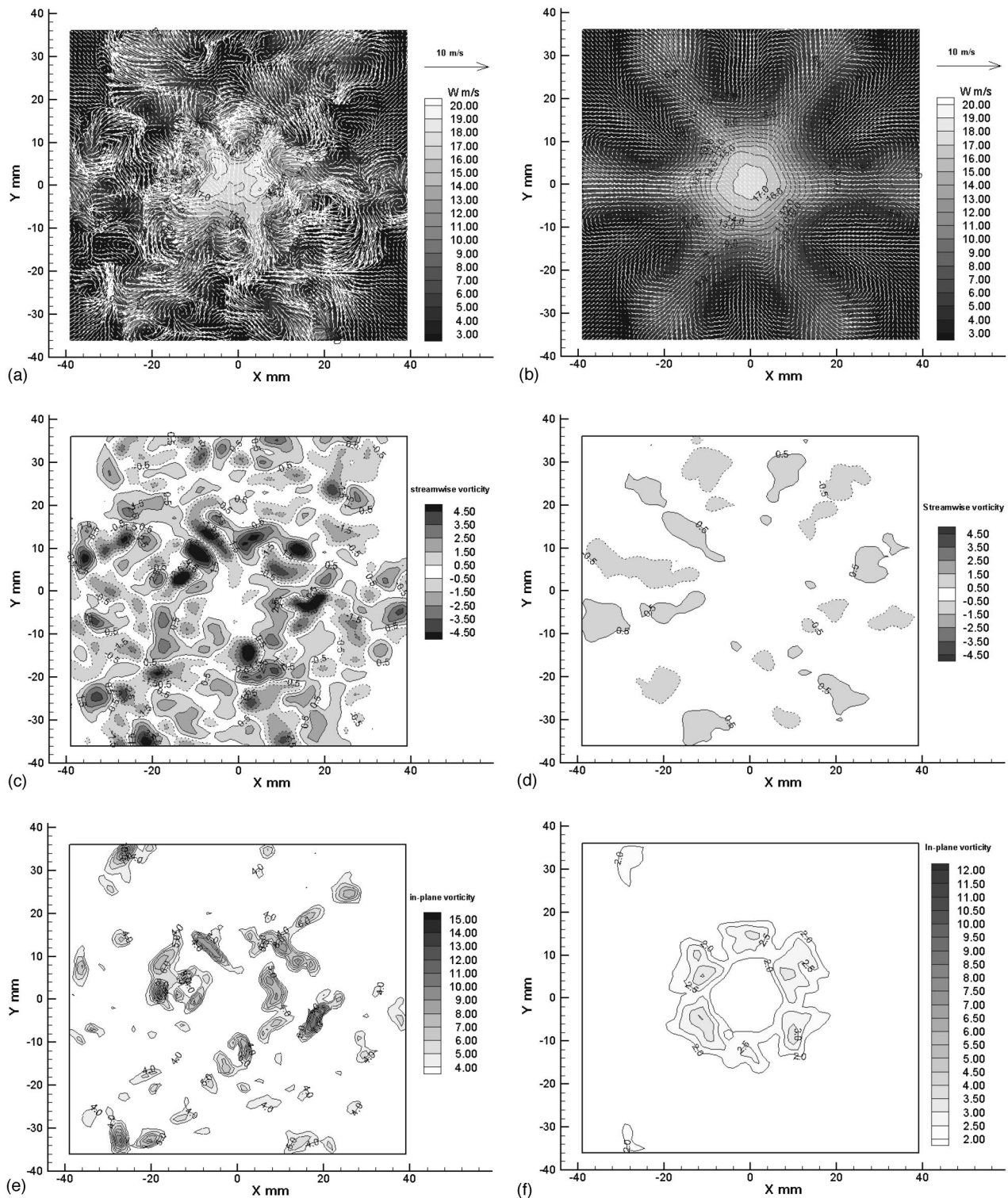


FIG. 6. The measurement results of the dual-plane stereoscopic PIV system in the $Z=80$ mm ($Z/D=2.0$) cross plane of the lobed jet flow. (a) Instantaneous velocity distribution, (b) ensemble-averaged velocity distribution, (c) simultaneous streamwise vorticity distribution, (d) ensemble-averaged streamwise vorticity distribution, (e) simultaneous azimuthal (in-plane) vorticity distribution, (f) ensemble-averaged azimuthal (in-plane) vorticity distribution.

clearly and quantitatively from the ensemble-averaged azimuthal vorticity distribution given in Fig. 5(f).

As the downstream distance increases to $Z=80$ mm ($Z/D=2.0$, $Z/H=5.33$), the lobed jet flow was found to become more and more turbulent. The “signature” of the lobed

nozzle in the form of “six-lobed structure” is almost indistinguishable in the instantaneous velocity field given in Fig. 6(a). The iso-velocity contours of the high-speed core jet flow were found to become small concentric circles in the ensemble-averaged velocity distribution [Fig. 6(b)]. The

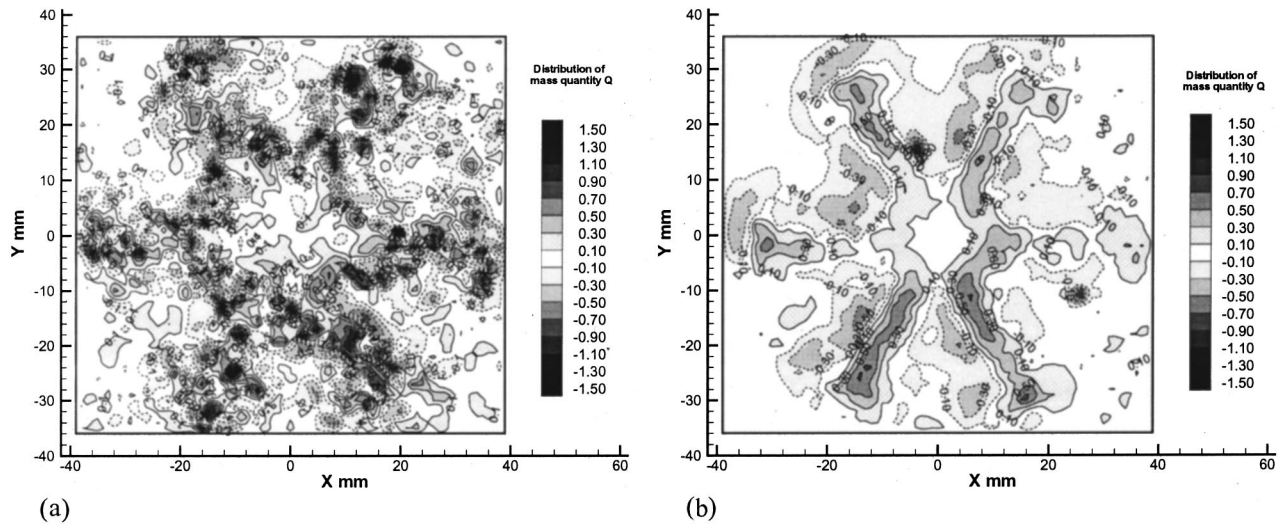


FIG. 7. A typical instantaneous and ensemble-averaged “mass quantity” Q distributions in the $Z=40$ mm cross plane of the lobed jet flow. (a) Instantaneous “mass quantity” Q distribution, (b) ensemble-averaged “mass quantity” Q distribution.

smaller instantaneous streamwise vortices originated from the breakdown of the large-scale streamwise vortices generated by the lobed nozzle almost fully filled the measurement window [Fig. 6(c)]. Since these instantaneous small-scale streamwise vortices are so unsteady that they appear very randomly in the flow field, only very vague vortical structures can be identified in the ensemble-averaged streamwise vorticity distribution [Fig. 6(d)]. The ensemble-averaged streamwise vorticity distribution also revealed that the ensemble-averaged streamwise vortices have been dissipated so seriously that their strength is only about one-eighth of those at the exit of the lobed nozzle. Due to the intensive mixing between the core jet flow and ambient flow, the broken azimuthal vortex tubes dissipated even more extensively. Only a few fragments of the broken azimuthal vortex tubes can be found from the instantaneous azimuthal vorticity distribution [Fig. 6(e)]. A circular-ring-like structure can be seen clearly in the center of the lobed jet flow from the ensemble-averaged azimuthal vorticity distribution given in Fig. 6(f).

The authors have suggested that the mixing enhancement caused by the special geometry of a lobed nozzle concentrates mainly within the first two diameters downstream of the lobed nozzle (first six lobe heights).^{13,14} The mixing between the core jet flow and ambient flow further downstream in a lobed jet flow will occur by the same gradient-type mechanism as that for a circular jet flow. The measurement results of the present dual-plane stereoscopic PIV system show that the azimuthal Kelvin–Helmholtz vortical rings and large-scale streamwise vortices broke down and dissipated very rapidly in the first two diameters of the lobed nozzle (first six lobe heights). Circular-ring-like structures were found further downstream in the lobed jet flow. These results are found to prove the conjectures suggested in the earlier work of the authors.^{13,14}

EVALUATION OF THE MEASUREMENT RESULTS BY USING MASS CONSERVATION EQUATION

It is well known that the equation

$$\frac{\partial u}{\partial x} + \frac{\partial v}{\partial y} + \frac{\partial w}{\partial z} = 0 \quad (6)$$

should be satisfied theoretically and automatically for an incompressible fluid flow, which is usually referred to as mass conservation equation.

Since a “classical” PIV system or a conventional stereoscopic PIV system only can provide measurement results of velocity vectors in one single plane, and the term of $\partial w/\partial z$ in the above mass conservation equation cannot be determined instantaneously. The satisfaction of the measurement results to the mass conservation equation cannot be checked. The present dual-plane stereoscopic PIV system can measure all three components of velocity vectors in two parallel planes instantaneously and simultaneously, and all the terms in the mass conservation equation (6) can be calculated instantaneously based on the measurement results of the present dual-plane stereoscopic PIV system.

A parameter named as “mass quantity” Q is introduced in the present study to quantify the satisfaction of the present dual-plane stereoscopic PIV measurement results to the mass conservation equation. The “mass” quantity Q is defined as

$$Q = \frac{D}{U_0} \left(\frac{\partial u}{\partial x} + \frac{\partial v}{\partial y} + \frac{\partial w}{\partial z} \right). \quad (7)$$

It should be noted that the “mass quantity” Q should be zero theoretically in order to satisfy the mass conservation equation (6). However, since any measurement result may be contaminated by measurement errors, and the “mass quantity” Q will not always be zero due to the measurement errors.

Figure 7(a) shows a typical instantaneous distribution of

the “mass quantity” Q based on the measurement results of the present dual-plane stereoscopic PIV system in the $Z = 40$ mm cross plane of the lobed jet flow. Based on 400 frames of the instantaneous results, the ensemble-averaged value of the “mass quantity” Q was calculated, which is given in Fig. 7(b). From the instantaneous and ensemble-averaged distributions of “mass quantity” Q , it can be seen that the value of “mass quantity” Q is not always zero over the measurement window due to measurement errors.

From both the instantaneous distribution and ensemble-averaged distribution of the “mass quantity” Q , it is found that the regions with bigger “mass quantity” Q always appear in the higher vorticity regions, where the shear motion is very serious. This may be explained by that since the accuracy level of the PIV results from the correlation-based PIV image procession method used in the present study is very sensitive to the shear motions in fluid flows. Therefore, bigger errors always appear in the regions with stronger shear motions.

Lawson and Wu¹⁶ suggested that the velocity error of the out-of-plane component (w_{error}) will be much bigger than those in the two in-plane components (u_{error} and v_{error}) when the half-view angle between the stereoscopic image recording cameras is less than 45° . In the present study, it is found that the largest source of the “mass quantity” Q always comes from the term of $\partial w/\partial z$. This result is considered to agree with the prediction of Lawson and Wu¹⁶ qualitatively since the half-angle between the stereoscopic image recording cameras of the present dual-plane stereoscopic PIV system is about 25° .

In order to quantify the measurement error levels of the dual-plane stereoscopic PIV measurement results more clearly, the measurement results of the present dual-plane stereoscopic PIV system are discomposed into accurate values and measurement errors, i.e., $u_{\text{measurement}} = u + u_{\text{error}}$; $v_{\text{measurement}} = v + v_{\text{error}}$; $w_{\text{measurement}} = w + w_{\text{error}}$. Then, Eq. (7) may be rewritten as

$$\begin{aligned} Q &= \frac{D}{U_0} \left(\frac{\partial u_{\text{measurement}}}{\partial x} + \frac{\partial v_{\text{measurement}}}{\partial y} + \frac{\partial w_{\text{measurement}}}{\partial z} \right) \\ &= \frac{D}{U_0} \left[\left(\frac{\partial u}{\partial x} + \frac{\partial v}{\partial y} + \frac{\partial w}{\partial z} \right) + \left(\frac{\partial u_{\text{error}}}{\partial x} + \frac{\partial v_{\text{error}}}{\partial y} + \frac{\partial w_{\text{error}}}{\partial z} \right) \right] \\ &= \frac{D}{U_0} \left(\frac{\partial u_{\text{error}}}{\partial x} + \frac{\partial v_{\text{error}}}{\partial y} + \frac{\partial w_{\text{error}}}{\partial z} \right). \end{aligned} \quad (8)$$

The terms of $\partial u_{\text{error}}/\partial x$, $\partial v_{\text{error}}/\partial y$, and $\partial w_{\text{error}}/\partial z$ in the above equation are recast into the finite difference form $\Delta u_{\text{error}}/\Delta x$, $\Delta v_{\text{error}}/\Delta y$, and $\Delta w_{\text{error}}/\Delta z$. A total velocity error ΔU_{error} is defined by $\Delta U_{\text{error}} = \Delta u_{\text{error}} + \Delta v_{\text{error}} + \Delta w_{\text{error}}$, and $\Delta x = \Delta y = \Delta z = 2$ mm for the present study. Then, Eq. (8) is rewritten as

$$Q = \frac{D}{U_0} \left(\frac{\Delta u_{\text{error}}}{\Delta x} + \frac{\Delta v_{\text{error}}}{\Delta y} + \frac{\Delta w_{\text{error}}}{\Delta z} \right) = \frac{D}{U_0} \cdot \frac{\Delta U_{\text{error}}}{\Delta z}. \quad (9)$$

It is assumed that the error in the derivative calculation mainly comes from the error in the velocity rather than the

distance. Then, the measurement error level ($\Delta U_{\text{error}}/U_0$) of the present dual-plane stereoscopic PIV measurement may be evaluated by

$$\frac{\Delta U_{\text{error}}}{U_0} = \frac{\Delta z Q}{D}. \quad (10)$$

For the typical instantaneous distribution of the “mass quantity” Q shown in Fig. 7(a), the maximum value of the “mass” quantity Q is about 1.5, i.e., $|Q_{\text{max}}| = 1.5$. The spatial-averaged absolute value of “mass quantity” Q over the whole measurement window is about 0.22, i.e.,

$$|Q|_{\text{spatial-averaged}} = \sum_{i=1}^{i=NI} \sum_{j=1}^{j=NJ} |Q_{i,j}| = 0.22.$$

According to Eq. (10), the error levels of the instantaneous measurement results of the present dual-plane stereoscopic PIV system may be

$$\left| \frac{\Delta U_{\text{error}}}{U_0} \right|_{\text{max}} = 7.5\% \quad \text{and} \quad \left| \frac{\Delta U_{\text{error}}}{U_0} \right|_{\text{spatial-averaged}} = 1.1\%.$$

For the ensemble-averaged value of the “mass quantity” shown in Fig. 7(b), the maximum value of the ensemble-averaged “mass quantity” Q is about 0.6, i.e., $|Q_{\text{ensemble-averaged}}|_{\text{max}} = 0.60$. The spatial-averaged absolute value of the ensemble-averaged “mass quantity” Q over the whole measurement window is about 0.12, i.e.,

$$\begin{aligned} |Q_{\text{ensemble-averaged}}|_{\text{spatial-averaged}} &= \sum_{i=1}^{i=NI} \sum_{j=1}^{j=NJ} |Q_{\text{ensemble-averaged},i,j}| \\ &= 0.12. \end{aligned}$$

Therefore, the error levels of the ensemble-averaged measurement results obtained by the present dual-plane stereoscopic PIV system may be $|(\Delta U_{\text{error}})_{\text{ensemble-averaged}}/U_0|_{\text{max}} = 3.0\%$, $|(\Delta U_{\text{error}})_{\text{ensemble-averaged}}/U_0|_{\text{spatial-averaged}} = 0.60\%$.

CONCLUSIONS

An advanced stereoscopic PIV system, which named as dual-plane stereoscopic PIV system, was described in the present paper to achieve simultaneous measurement of all three components of the velocity and vorticity vector fields in a fluid flow. The dual-plane stereoscopic PIV system uses the polarization conservation characteristic of Mie scattering to achieve simultaneous stereoscopic PIV measurements at two spatially separated planes. The objective fluid flow was illuminated with two orthogonally linearly polarized laser sheets at two spatially separated planes. The light scattered by the tracer particles in the two illuminating laser sheets with orthogonal linear polarization were separated by using polarizing beam splitter cubes, then recorded separately by using high resolution CCD cameras. A 3D *in situ* calibration procedure was used to determine the relationships between the two-dimensional image planes and three-dimensional object fields for both position mapping and velocity three-component reconstruction. Unlike “classical” PIV systems or single-plane stereoscopic PIV systems, which can only get one-component of vorticity vectors, the dual-plane stereo-

scopic PIV system can provide all three components of the velocity and vorticity vector distributions instantaneously and simultaneously.

The dual-plane stereoscopic PIV system was used to conduct measurement in an air jet flow exhausted from a lobed nozzle. The large-scale streamwise vortices generated by the lobed nozzle and azimuthal vortical structures due to the Kelvin–Helmholtz instability in the lobed jet flow were revealed simultaneously and quantitatively from the measurement results of the dual-plane stereoscopic PIV system. The evolution and interaction characteristics of the large-scale streamwise vortices and azimuthal Kelvin–Helmholtz vortices in the lobed jet flow were discussed based on the simultaneous measurement results. A discussion about the satisfaction of the measurement results of the present dual-plane stereoscopic PIV system to the mass conservation equation was also conducted to evaluate the error levels of the measurement results.

- ¹R. J. Adrian, “Particle-image technique for experimental fluid mechanics,” *Annu. Rev. Fluid Mech.* **23**, 261 (1991).
²A. K. Prasad, “Stereoscopic particle image velocimetry,” *Exp. Fluids* **29**, 103 (2000).
³E. McCartney, *Optics of the Atmosphere: Scattering by Molecules and Particles* (Wiley, New York, 1976).
⁴C. C. Landreth and R. J. Adrian, “Electrooptical image shifting for particle image velocimetry,” *Appl. Opt.* **27**, 4216 (1988).

- ⁵C. J. Kaehler and J. Kompenhans, “Multiple plane stereo PIV: Technical realization and fluid-mechanical significance,” *Proceedings of the Third International Workshop on PIV*, Santa Barbara, 16–18 September 1999.
⁶A. K. Prasad and K. Jensen, “Scheimpflug stereocamera for particle image velocimetry in liquid flows,” *Appl. Opt.* **34**, 7092 (1995).
⁷S. M. Soloff, R. J. Adrian, and Z. C. Liu, “Distortion compensation for generalized stereoscopic particle image velocimetry,” *Meas. Sci. Technol.* **8**, 1441 (1997).
⁸H. Hu, T. Saga, T. Kobayashi, N. Taniguchi, and S. Segawa, “The spatial resolution improvement of PIV result by using hierarchical recursive operation,” *Proceedings of 9th International Symposium on Flow Visualization*, Edinburgh, Scotland, UK, 22–25 August 2000.
⁹H. Hu, T. Saga, T. Kobayashi, N. Taniguchi, and M. Yasuki, “Dual-plane stereoscopic particle image velocimetry: System setup and its application on a lobed jet mixing flow,” *Exp. Fluids* **31**, 277 (2001).
¹⁰H. Hu, Ph.D. thesis, University of Tokyo, Tokyo, Japan, 2001.
¹¹D. C. McCormick and J. C. Bennett, “Vortical and turbulent structure of a lobed mixer free shear layer,” *AIAA J.* **32**, 1852 (1994).
¹²V. M. Belovich and M. Samimy, “Mixing process in a coaxial geometry with a central lobed mixing nozzle,” *AIAA J.* **35**, 838 (1997).
¹³H. Hu, T. Saga, T. Kobayashi, and N. Taniguchi, “Research on the vortical and turbulent structures in the lobed jet flow by using LIF and PIV,” *Meas. Sci. Technol.* **11**, 698 (2000).
¹⁴H. Hu, T. Saga, T. Kobayashi, and N. Taniguchi, “A study on a lobed jet mixing flow by using stereoscopic particle image velocimetry technique,” *Phys. Fluids* **13**, 3425 (2001).
¹⁵A. Melling, “Tracer particles and seeding for particle image velocimetry,” *Meas. Sci. Technol.* **8**, 1406 (1997).
¹⁶N. J. Lawson and J. Wu, “Three-dimensional particle image velocimetry: Error analysis of stereoscopic techniques,” *Meas. Sci. Technol.* **8**, 894 (1997).